Nuclear Engineering and Technology 54 (2022) 2395–2407

Contents lists available at ScienceDirect

Nuclear Engineering and Technology

journal homepage: www.elsevier.com/locate/net

Original Article

Application of the SCIANTIX fission gas behaviour module to the integral pin performance in sodium fast reactor irradiation conditions

A. Magni [a], D. Pizzocri [a], L. Luzzi [a, *], M. Lainet [b], B. Michel [b]

[a] Politecnico di Milano, Department of Energy, Nuclear Engineering Division, via La Masa 34, 20156, Milano, Italy
[b] Commissariat à l'Energie Atomique et aux Energies Alternatives, CEA DEC/SESC, 13108, St. Paul Lez Durance, France

ARTICLE INFO

Article history:
Received 12 October 2021
Received in revised form
30 January 2022
Accepted 4 February 2022
Available online 5 February 2022

Keywords:
ASTRID case study
Fuel pin performance
Fission gas behaviour
SCIANTIX
GERMINAL
TRANSURANUS
Burst release

ABSTRACT

The sodium-cooled fast reactor is among the innovative nuclear technologies selected in the framework of the development of Generation IV concepts, allowing the irradiation of uranium-plutonium mixed oxide fuels (MOX). A fundamental step for the safety assessment of MOX-fuelled pins for fast reactor applications is the evaluation, by means of fuel performance codes, of the integral thermal-mechanical behaviour under irradiation, involving the fission gas behaviour and release in the fuel-cladding gap. This work is dedicated to the performance analysis of an inner-core fuel pin representative of the ASTRID sodium-cooled concept design, selected as case study for the benchmark between the GERMINAL and TRANSURANUS fuel performance codes. The focus is on fission gas-related mechanisms and integral outcomes as predicted by means of the SCIANTIX module (allowing the physics-based treatment of inert gas behaviour and release) coupled to both fuel performance codes. The benchmark activity involves the application of both GERMINAL and TRANSURANUS in their "pre-INSPYRE" versions, i.e., adopting the state-of-the-art recommended correlations available in the codes, compared with the "post-INSPYRE" code results, obtained by implementing novel models for MOX fuel properties and phenomena (SCIANTIX included) developed in the framework of the INSPYRE H2020 Project. The SCIANTIX modelling includes the consideration of burst releases of the fission gas stored at the grain boundaries occurring during power transients of shutdown and start-up, whose effect on a fast reactor fuel concept is analysed. A clear need to further extend and validate the SCIANTIX module for application to fast reactor MOX emerges from this work; nevertheless, the GERMINAL-TRANSURANUS benchmark on the ASTRID case study highlights the achieved code capabilities for fast reactor conditions and paves the way towards the proper application of fuel performance codes to safety evaluations on Generation IV reactor concepts.

1. Introduction

The sodium-cooled fast reactor (SFR) is among the innovative nuclear technologies selected in the framework of the Generation IV reactor concept development [1,2]. Gen-IV systems (liquid metal-cooled) are designed as fast reactors (FRs) employing fuel pins composed of uranium-plutonium mixed-oxide fuel (MOX) wrapped in stainless-steel cladding materials (e.g., cold-worked 15-15Ti). A fundamental step for the design of MOX fuel pins for Gen-IV irradiation is the prediction of their integral thermal-mechanical performance under fast neutron spectrum and related safety assessment by means of fuel performance codes, in order to verify the compliance of the simulation outcomes with dedicated design limit criteria. The objective of this work is indeed to analyse the behaviour under nominal irradiation of an inner-core fuel pin representative of the ASTRID (Advanced Sodium Technological Reactor for Industrial Demonstration) SFR design [3,4], selected as case study for the benchmark between the GERMINAL [5,6] and TRANSURANUS [7,8] fuel performance codes. The fission gas behaviour and release in the fuel-cladding gap is pivotal in impacting the overall pin performance with increasing fuel burn-up, since it represents a potential limiting-life factor for

* Corresponding author.
E-mail address: lelio.luzzi@polimi.it (L. Luzzi).

https://doi.org/10.1016/j.net.2022.02.003

the pin in-reactor permanence [9] and hence needs to be targeted by dedicated modelling efforts. To this end, a particular focus here is on the physics-based modelling and simulation of fission gas-related mechanisms by means of the SCIANTIX grain-scale module [10], allowing the coherent treatment of inert gas behaviour and release obtained from the intra- and inter-granular dynamics and coupled to both fuel performance codes [11].

The fuel pin design selected in this study corresponds to the ASTRID French 600 MWe sodium-cooled fast reactor demonstrator at the end of its Conceptual Design phase in 2015 [3]. The core design studies have been conducted by the CEA (Commissariat à l'énergie atomique et aux énergies alternatives) with support from AREVA and EDF (Électricité de France). Innovative core design choices have been made to comply with the Gen-IV reactor targets, thereby marking a break with the former Phénix and SuperPhénix French SFRs [3,12]. The main objective of improving the safety levels compared to current Gen-II or Gen-III reactors has led to a core design featuring an intrinsically safe behaviour in transients of accidental conditions. In line with the technological solutions employed to increase the ASTRID concept safety, the specific fuel pin design consists in annular fissile pellets and a heterogeneous axial composition of the fuel column (i.e., an alternation of fissile and fertile axial zones) [13]. These design characteristics are related to the margin to fuel melting (benefiting from annular pellets) and to the CFV (Coeur à Faible effet de Vide) core design corresponding to a negative or null sodium void reactivity effect [4,14].

The objective of this work is thus to assess the ASTRID fuel pin behaviour in normal operation conditions by means of two fuel performance codes (FPCs), TRANSURANUS and GERMINAL, whose capabilities towards FR fuel and irradiation conditions have been extended in the framework of the INSPYRE H2020 Project [15]. The first step of the benchmark activity consisted in applying the reference versions of both codes, prior to the modelling extensions performed. Then, as a second step, the integral impact on the ASTRID case study [16] of the advancements achieved during the INSPYRE Project is discussed, particularly for what concerns the mechanistic modelling of fission gas behaviour in oxide fuels brought about by the coupling of both FPCs with the SCIANTIX module. This joint activity is reflected in this paper, including a detailed analysis of the effect on fission gas release of fuel micro-cracking during operational power transients, providing burst releases of gas in the fuel-cladding gap [17]. The engineering simulation outcomes addressed in this study concern mainly the fuel maximal temperature, the evolution of the fuel-cladding gap and the cladding deformation at the end of irradiation, driven by fuel-cladding mechanical interaction at gap closed but influenced also by fission gas release and related pin inner pressure. The heat transfer through the fuel-cladding gap and the degree of gap composition pollution by fission gas release have a first-order effect on the fuel temperature and on the fuel pin inner pressure, relevant for two main design limits typically adopted for the pin safe irradiation, i.e., the margin to fuel melting and an absent/limited cladding visco-plastic strain (ensuring the cladding integrity as a first barrier against the release of radioactive fission products) [18].

The paper is structured as follows. Section 2 is dedicated to a recall of the current capabilities of the SCIANTIX fission gas behaviour module and of its coupling with the GERMINAL and TRANSURANUS fuel performance codes. The ASTRID case study considered in this work, including the specifications of the inner-core fuel pin and irradiation history, is described in Section 3, while Section 4 collects the main results of the code benchmark in terms of relevant engineering quantities and fission gas-related outcomes. A deeper analysis of the effect of the model for fission gas burst releases implemented in SCIANTIX is provided in Section 5. Conclusions are drawn in Section 6 together with further developments of this work.

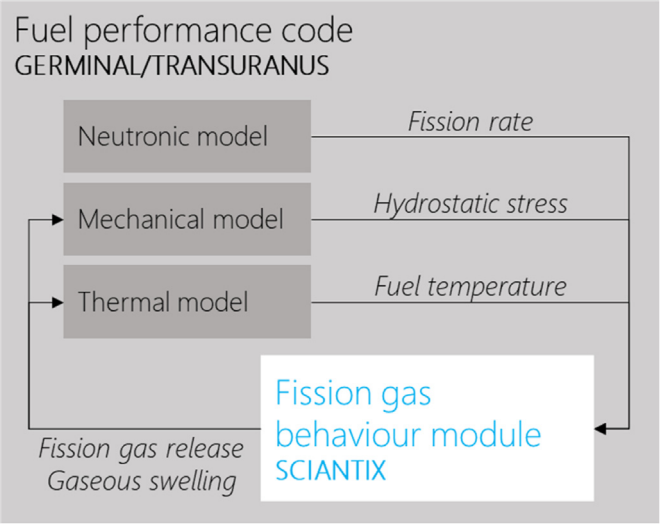

Fig. 1. Sketch of the coupling scheme between GERMINAL/TRANSURANUS and SCIANTIX.

2. SCIANTIX application as fission gas behaviour module

SCIANTIX is an open-source code devoted to the physics-based modelling of inert gas behaviour at the grain-scale [10,19]. It includes rate-theory models for the description of intra- and inter-granular gas behaviour [17,20,21], for both fission gases and helium [22,23].[1] The architecture of SCIANTIX is designed to ease coupling with fuel performance codes, in which SCIANTIX plays the role of fission gas behaviour module. Currently, its coupling has been setup in TRANSURANUS, GERMINAL (for both codes, in the frame of the INSPYRE Project [11,15]), and OFFBEAT [24,25].

This section aims at describing the integration of SCIANTIX in TRANSURANUS and GERMINAL, applied to the simulation of the ASTRID case study (Sections 3 and 4). For both fuel performance codes, the coupling scheme involves the call of SCIANTIX at each mesh point, during each time-step, and at each convergence iteration. For each of these calls, SCIANTIX updates the physics-based variables related to inert gas behaviour, either internally or by transferring the updates to the external fuel performance code. The general flow of information between the two fuel performance codes and SCIANTIX is sketched in Fig. 1, with SCIANTIX receiving as inputs the local fuel temperature, the local fission rate, the local hydrostatic stress, and the time-step, and providing as outputs the local contribution to the integral fission gas release and the local gaseous swelling. These two outputs are directly connected to the overall thermal-mechanical behaviour of the fuel pin.

As for the GERMINAL//SCIANTIX coupled suite, the coupling has been achieved by introducing the module for fission gas behaviour in the multi-physics convergence loop for each of the considered axial slice of the fuel pin. The main improvements expected from the coupling concern the simulation of the fuel pin behaviour at intermediate power levels. As GERMINAL is devoted to the simulation of fast reactor fuel pins [5,6], for which fission gas release is typically high, the inclusion of SCIANTIX is expected to play a role in the early and intermediate stages of irradiation, i.e., while fission

[1] It is out of the scope of this work to present an in-depth description of the models available in SCIANTIX, for which the reader is referred to Refs. [10,36].

gas release is not preponderant. Consequently, it is critical to evaluate it as precisely as possible since it is physically linked to the contribution of gas swelling to the geometrical evolution of the fuel pellet. From the fuel temperature point of view, the simulation of the behaviour at the fuel pin extremities, where the fuel is colder and therefore the kinetics of fission gas diffusion is slower, is expected to benefit from the inclusion of the SCIANTIX module.

As for the TRANSURANUS//SCIANTIX coupling, SCIANTIX has been added to the available options for fission gas behaviour modelling of TRANSURANUS, able to target both thermal and fast reactor irradiation conditions [8]. The module is therefore called at each point of the fine radial grid of the TRANSURANUS discretization, at each node of the fuel axial discretization [7].

Preliminary testing of GERMINAL//SCIANTIX and TRANSURANUS//SCIANTIX identified model adjustments required for the reliable application of SCIANTIX to fast reactor conditions:

- The grain size evolution (i.e., the fuel micro-structure) during irradiation is currently estimated using temperature-dependent empirical correlations, such as that proposed by Sari [26] in GERMINAL or the model by Ainscough [27] (reviewed by Botazzoli et al. [28,29]) in TRANSURANUS. These correlations tend to overestimate the grain size in the hot (central) regions of the fuel, whereas SCIANTIX requires sound values of the grain size to model the intra-granular gas diffusion process. For these reasons, upper bounds for the grain growth in the different radial zones of the fuel pellets – columnar grains zone, equiaxed grain zone, un-restructured zone – have been introduced in GERMINAL. These bounds impact the gaseous swelling by affecting the grain surface-to-volume ratio, connected to the gas storing capacity of the grain boundaries [21,30].
- The model governing the growth and interconnection of grain boundary bubbles currently available in SCIANTIX is tailored and validated for application to light water reactor conditions [10,21]. In fast reactor conditions, where fuel temperatures tend to be higher, an upper limit to the size of grain boundary bubbles has been introduced. This limit is numerically in line with the development proposed to handle a similar problem in the BISON code [30].
- The SCIANTIX solver for intra-granular diffusion has been adapted to handle the coupled evolution of the fission gas in solution and in intra-granular bubbles [31,32], overcoming the quasi-stationary assumption [33,34].
- The state-of-the-art gas diffusivity by Turnbull [35] has been extended with a thermally-activated term saturating faster (hyperbolic tangent-shaped) and hence limiting the diffusivity at high temperature. This contribution is intended to compensate the observed dominance of the intra-granular bubble trapping rate at high temperatures when compared to the bubble re-solution rate.
- The treatment of the open paths for fission gas release, determined by the SCIANTIX modelling of burst releases [17], is subject to an artifact associated to the current implementation of the burst release model in the GERMINAL code. After the occurrence of sudden (burst) releases of the inter-granular fission gas during the power transients of shutdown and start-up (corresponding to the ASTRID reactor inter-cycles), the fission gas release is limited during the following power cycle until the threshold for the storing capability of the grain boundaries is reached again (which, if happening during a power cycle of normal operation, triggers the fission gas release again).

All the above-mentioned modifications of the standard SCIANTIX models have been implemented in the GERMINAL//SCIANTIX coupled suite, whereas SCIANTIX has been coupled to TRANSURANUS preserving the SCIANTIX original modelling features. When applying TRANSURANUS//SCIANTIX, the impact of the TRANSURANUS grain growth model and of the SCIANTIX modelling of burst releases of fission gases (detailed in Section 5) coupled to TRANSURANUS have been explicitly considered in the following analyses (Section 4).

3. Description of the ASTRID applicative case study

The ASTRID fuel pin concept is based on an axially heterogeneous fuel column (i.e., active column composed by fertile and fissile axial zones) and annular fissile pellets. Table 1 reports the geometry and pin specifications of an inner-core fuel pin representative of the ASTRID design [16]. The cladding material is an austenitic stainless steel 15-15Ti (15% Cr, 15% Ni, 0.45% Ti) and the fuel is made of uranium-plutonium mixed oxides for what concerns the fissile pellets, while the fertile pellets are made of uranium dioxide. Fig. 2 reports a schematic of the fuel pin section.

The scenario herein considered consists in the nominal irradiation at the ASTRID operative power of 1500 MW_{th}. The sodium inlet temperature is assumed to be constant and equal to 400°C, with a pressure of 0.3 MPa. The sodium mass flow rate per pin is also assumed constant and equal to 0.1 kg s^{-1}. The fuel residence time is of 1440 EFPD (Equivalent Full Power Days), divided in four cycles of 360 EFPD each, with a progressive linear power decrease of 10% up to the end of irradiation. The irradiation history of the inner-core ASTRID pin (based on [4,13] and shown in Fig. 3) presents a maximum linear heat rate of $q' = 46.3$ kW m^{-1} at the beginning of irradiation (i.e., after the first power rise at reactor start-up). The total neutron flux ϕ is defined as proportional to the linear heat rate, i.e., ϕ (neutrons cm^{-2} s^{-1}) $= 7.31 \cdot 10^{13}\, q'$ (kW m^{-1}), in order to be consistent with the end-of-life cladding dose of 110 dpa NRT(Fe) given in Ref. [13].

As for the cladding damage, it is assumed that 70% of the neutron flux has an energy above 0.111 MeV and is hence considered as fast. The axial shape factors for both the linear heat rate and the fast neutron flux are reported in Table 2 and the corresponding profile is shown in Fig. 4 [13].

The objective of this benchmark activity between TRANSURANUS and GERMINAL on the ASTRID concept is to simulate and compare the predicted behaviour of a hot-channel (inner-core) fuel

Table 1
Design parameters of the ASTRID inner-core fuel pin.

Parameter	Value
Lower fertile zone height (mm)	300
Lower fissile zone height (mm)	250
Inner fertile zone height (mm)	200
Upper fissile zone height (mm)	350
Lower plenum length (mm)	800
Upper plenum length (mm)	80
Inner diameter, fissile pellets (mm)	2.45
Fuel outer diameter (mm)	8.46
Cladding inner diameter (mm)	8.70
Cladding outer diameter (mm)	9.70
Wire spacer diameter (mm)	1
Filling gas (He) pressure (MPa)	0.1
Fuel grain size (μm)	10
Porosity (%)	5
O/M, fissile pellets	1.97
O/M, fertile pellets[a]	2.00
Pu/M, fissile pellets[b]	0.23
Peak fuel burn-up at the end of irradiation (GWd t_{HM}^{-1})	137.2

[a] UO_2, U-natural.
[b] Pu-238/Pu = 0.23%, Pu-239/Pu = 67.87%, Pu-240/Pu = 26.07%, Pu-241/Pu = 4.62%, Pu-242/Pu = 1.2% (wt.%).

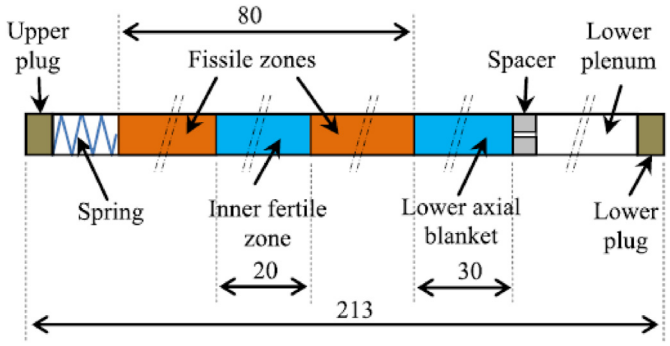

Fig. 2. Schematic of an ASTRID inner-core fuel pin (dimensions in cm) [3].

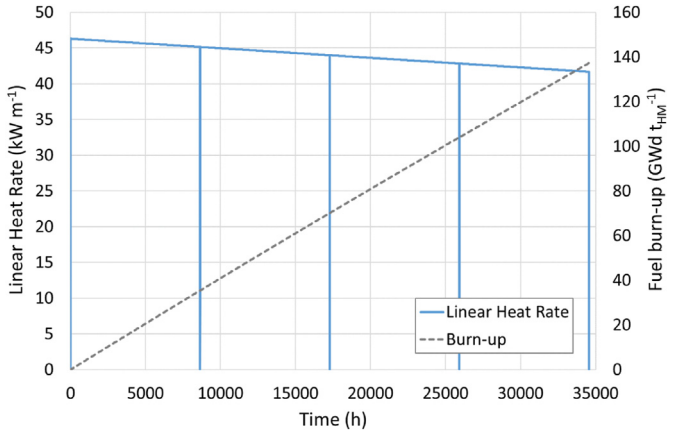

Fig. 3. Linear heat rate evolution for the ASTRID inner-core fuel pin at the axial peak power node, based on [13]. The evolution of the peak fuel burn-up (i.e., at the peak power node, average on the section) is included on the secondary vertical axis.

Table 2
Peak factors defining the axial profiles of the linear power and fast neutron flux of the ASTRID inner-core pin, based on [13].

Axial position from bottom of fuel column (cm)	Shape factor (/)	Pellet type
104.17	0.8460	Fissile
92.50	0.9945	Fissile
80.83	0.9293	Fissile
70.00	0.0509	Fertile
60.00	0.0416	Fertile
50.83	0.5807	Fissile
42.50	0.5270	Fissile
34.17	0.4253	Fissile
25.00	0.0208	Fertile
15.00	0.0069	Fertile
5.00	0.0000	Fertile

pin under nominal irradiation, to assess the code capabilities on a sodium-cooled fast reactor case study representative of Generation IV conditions. The focus of the analysis of the simulation results is particularly on the fission gas behaviour as predicted by the physics-based SCIANTIX module coupled to both GERMINAL and TRANSURANUS ([11] and as outlined in Section 2), highlighting the modelling novelties with respect to the state-of-the-art approach adopted by the two fuel performance codes. Indeed, the code-to-code benchmark involves also the application of the extended FPC versions (inclusive of the coupling with SCIANTIX), herein labelled "post-INSPYRE", to show the impact on the pin performance results of the modelling improvements for MOX fuel

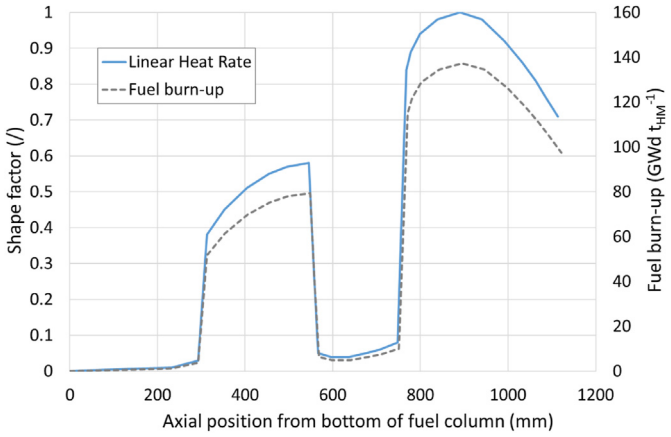

Fig. 4. Graphical representation of the axial profiles of linear power and fast neutron flux of the ASTRID inner-core pin, relative to their respective maximum values, based on [13]. The axial profile of the fuel burn-up at the end of irradiation (average on the sections) is included on the secondary vertical axis.

properties and behaviour developed in the framework of the INSPYRE Project [15]. In particular, the INSPYRE modelling activities concerned three main areas of properties/phenomena:

- Fission gas and helium behaviour in MOX, implemented in the SCIANTIX module [10,36].
- MOX mechanical properties: thermal expansion, Young's modulus [11,37].
- MOX thermal properties: thermal conductivity, melting temperature [38,39].

In the following Section 4, the effect of the novel INSPYRE models on the integral ASTRID pin behaviour is discussed in relation to selected figures of merit. The standard "pre-INSPYRE" code results (prior to the modelling developments achieved in the INSPYRE framework) are compared to the "post-INSPYRE" ones, corresponding to the extended code versions as outlined in Ref. [11] (i.e., employing the above-mentioned novel INSPYRE recommendations instead of the code reference ones, and the coupling with the SCIANTIX inert gas behaviour module). The impact of the novel correlations for the MOX thermal and mechanical properties alone on the simulation results is provided, aiming at decoupling it as much as possible from the effect of the mechanistic modelling of fission gas behaviour brought about by SCIANTIX. Moreover, additional model sensitivity analyses have been performed with TRANSURANUS on the fuel grain growth, relevant for the fission gas behaviour (input for the SCIANTIX module) and driving specific pin performance outcomes, i.e., the fission gas release in the fuel-cladding gap and related pin inner pressure. Therefore, the figures presented and discussed in Section 4 include further TRANSURANUS results, herein labelled as:

- "pre-INSPYRE w/new MOX properties": results obtained with the same settings of the "pre-INSPYRE" simulation, but employing the novel correlations for thermal and mechanical properties of MOX fuel [11,37–39] instead of the code standard models.
- "post-INSPYRE w/o grain growth": results obtained with the same settings of the "post-INSPYRE" simulation, but without considering the fuel grain growth process.

It is worth underlining the different "post-INSPYRE" strategies adopted by GERMINAL and TRANSURANUS, reflecting on the

results presented in the following Section 4. The post-INSPYRE GERMINAL code already adopts the SCIANTIX burst release model [17], while in the post-INSPYRE TRANSURANUS calculations this model is not directly employed: it is activated separately to show its impact on the fission gas release and gap pressure. Moreover, the "pre-INSPYRE w/new MOX properties" set-up of the GERMINAL code has been also tested on the ASTRID case study, revealing differences with the pre-INSPYRE simulation results lower than 1%. This indicates that the standard GERMINAL models (prior to the modelling advancements for fast reactor MOX fuels achieved during the INSPYRE Project [11]) prove already well suitable in reproducing the herein considered thermal-mechanical properties of FR fuels (GERMINAL is indeed a fuel performance code historically tailored for FR simulations [5]). For this reason, the corresponding curves have not been added in the following Fig. 5 – 12, being consistent with the pre-INSPYRE ones.

4. Integral pin performance results and discussion

The simulation outcomes on the ASTRID inner-core fuel pin are provided in the figures of this Section, showing side by side the GERMINAL results (left) and the TRANSURANUS ones (right).

4.1. Evolutions in time: fuel-cladding gap width and fuel central temperature

As shown in Fig. 5, the fuel-cladding radial gap width predicted by GERMINAL (both pre- and post-INSPYRE versions) is subjected to a fast closure at the beginning of the first cycle (after ~ 400 h of irradiation). The gap re-opens at the end of the second cycle due to the formation of the Joint Oxyde-Gaine (JOG [5]), corresponding to an additional layer of fission product compounds evolving between the fuel and the cladding at sufficiently high fuel burn-up. The evolution of the gap size resulting from the post-INSPYRE settings is different after gap re-opening (i.e., a thinner JOG layer forms), due to a lower amount of caesium release predicted by the SCIANTIX module (the caesium release is correlated to the xenon and krypton release [5], here referring to the release predicted by SCIANTIX in the coupled suite GERMINAL//SCIANTIX).

Instead, TRANSURANUS predicts a slower fuel-cladding gap closure during the first irradiation cycle (closing after around 5000 h of irradiation), which contributes to higher predicted temperatures compared to GERMINAL, as shown by the following Fig. 6. Apart from the sudden gap re-openings due to pin structure relaxation caused by power shutdowns, the gap keeps always closed from the second power cycle on (no gap re-opening as from GERMINAL occurs, since e.g., the JOG layer in the fuel-cladding gap of FR pins is presently not accounted for by TRANSURANUS). The differences in the TRANSURANUS predictions of the gap size brought about by the novel INSPYRE models are generally significant only at the beginning of irradiation (when the gap is still open). The gap closure is faster during the first cycle (after the initial start-up power increase where the fuel thermal expansion dominates), mainly due to an enhanced fuel swelling predicted by the SCIANTIX module involved in the post-INSPYRE simulation [10]. Indeed, the novel correlations for the MOX thermal-mechanical properties alone [11,37–39] prove to have a limited impact on the gap width with respect to the pre-INSPYRE TRANSURANUS results. The fastest gap closure is obtained by switching off the fuel grain growth, which can be explained with a higher release of fission gases at the grain boundaries contributing to the inter-granular fuel swelling. The smallest fuel-cladding residual gap emerging from this simulation case (before gap closure) reflects on the lowest fuel central temperature at beginning of irradiation.

For what concerns the evolution in time of the fuel central temperature at the axial peak power node (Fig. 6), the highest value according to the pre-INSPYRE code versions is reached at the beginning of the first irradiation cycle (just after the first power increase – reactor start-up) and is equal to 2280°C according to GERMINAL and 2105°C according to TRANSURANUS. The fuel central temperature predicted by GERMINAL (Fig. 6 – left) rapidly decreases at the beginning of irradiation due to the fast fuel-cladding gap closure (Fig. 5 – left), followed by a slower decrease during the first cycle due to the fuel central hole extension induced by radial migration of porosity (as reported by Fig. 4, the peak power node is located in the upper fissile zone of the column, where an initial fuel inner radius is present in the as-fabricated pellets). Instead, the fuel central temperature according to pre-INSPYRE TRANSURANUS decreases more slowly, but still it can be related to the fuel progressive swelling leading to gap closure, although with different dynamics with respect to GERMINAL (Fig. 5 – right). From the second cycle on, the temperature increase predicted by pre-INSPYRE GERMINAL is mainly driven by the degradation of fuel thermal conductivity and gap conductance (due to fuel burn-up and pollution of the gap composition caused by fission gas release, respectively), partially compensated by the beneficial effect of the oxygen-to-metal ratio increase towards fuel stoichiometry (i.e., O/M = 2.00) and the power decrease. The same kind of analysis holds for the pre-INSPYRE TRANSURANUS calculation, although the beneficial thermal effect of gap closure on the fuel temperature regime prevails. The fuel thermal conductivity is modelled by both pre-INSPYRE codes with the Philipponneau's correlation [40] for the MOX fissile pellets. The sudden fuel temperature decrease predicted by GERMINAL at the end of the second

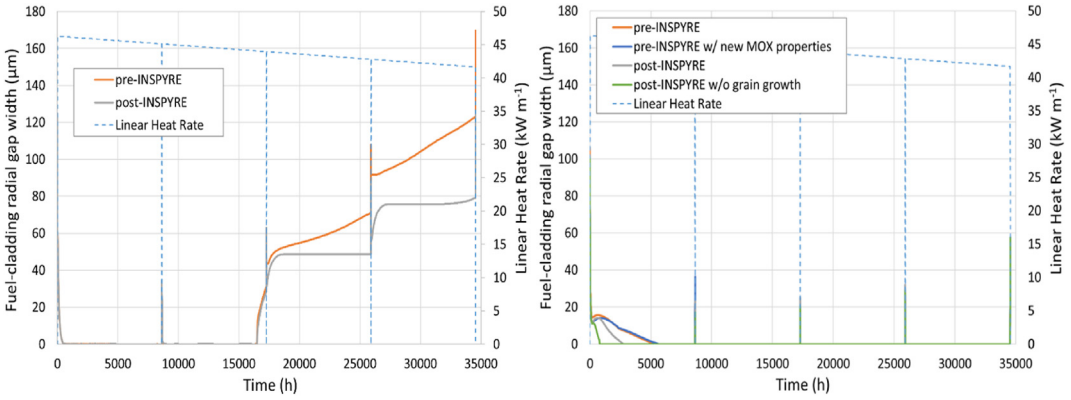

Fig. 5. Fuel-cladding gap width evolution at the peak power node, as predicted by GERMINAL (left) and TRANSURANUS (right).

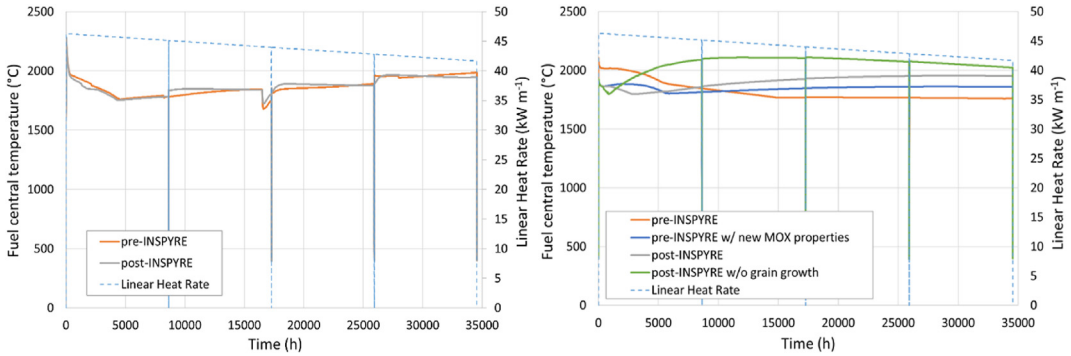

Fig. 6. Fuel central temperature evolution at the peak power node, as predicted by GERMINAL (left) and TRANSURANUS (right).

irradiation cycle is linked to the JOG formation, which improves the fuel-cladding gap conductance [5] (not accounted for at present by the TRANSURANUS code).

The post-INSPYRE version of GERMINAL leads to a similar result in terms of maximal fuel central temperature reached at the beginning of irradiation, and the evolution during the irradiation cycles shows only slight differences with the pre-INSPYRE calculation results. These discrepancies are supposedly ascribable to a different treatment of the fission gas behaviour in SCIANTIX [10,36] (involved in the post-INSPYRE code strategy) leading to a different fuel swelling and gas release from the fuel pellets impacting on the gap conductance and hence on the fuel temperature regime (Fig. 6 – left). Moreover, a correlation between the trends of gap width (after its re-opening due to JOG formation and evolution) and of the fuel central temperature can be noticed, since the latter increases as the gap width increases from the pre-INSPYRE simulation, while it remains almost constant like the fuel-cladding gap size from post-INSPYRE GERMINAL. For what concerns TRANSURANUS, the post-INSPYRE outcome is an increasing fuel central temperature already from the first irradiation cycle, as from GERMINAL but mostly driven by the burn-up degradation of the thermal conductivity represented by the novel correlation [38], despite the closure of the fuel-cladding gap. The introduction of the novel correlation for the MOX thermal conductivity [38] provides more aligned results between the post-INSPYRE codes at least in terms of fuel central temperature dynamics (Fig. 6). The additional sensitivity analysis performed with post-INSPYRE TRANSURANUS (i.e., switching off the fuel grain growth model) reveals a sensibly lower fuel temperature reached as a consequence of the first power increase (Fig. 6 – right), due to the combined effect of a higher fuel thermal conductivity at beginning of irradiation [38] and a higher fuel swelling from SCIANTIX [10] causing faster gap closure. After these initially dominant effects, the prevented fuel grain growth provides the highest fuel temperature regime during the intermediate cycles, determined by the enhanced degradation of both fuel thermal conductivity (due to the effect of the porosity and intergranular gas dynamics predicted by SCIANTIX [10]) and gap conductance due to a higher amount of fission gas release than in the post-INSPYRE case. The "post-INSPYRE w/o grain growth" simulation case corresponds to the maximum fuel central temperature, reached at the beginning of the third power cycle and equal to 2110°C, only slightly higher than the beginning-of-irradiation one according to pre-INSPYRE TRANSURANUS and still not of concern for the safety margin to fuel melting. The TRANSURANUS post-INSPYRE simulation strategies lead to higher temperatures at the end of irradiation, i.e., ~ 2000°C compared to ~ 1760°C from the pre-INSPYRE code version.

4.2. Evolutions in time: fission gas release and pin inner pressure

Figs. 7 and 8 show the evolutions in time of the integral fission gas release (FGR) and of the pin inner pressure, respectively. From both codes (and both pre- and post-INSPYRE versions), the pin pressure progressively increases as the FGR leads to an accumulation of gas in the fuel pin free volume. Nevertheless, the dynamics and final values reached are sensibly different, although consistent between pressure and FGR for each code.

According to pre-INSPYRE GERMINAL, both evolutions of inner pressure and FGR smoothly increase as fuel irradiation proceeds, up to final values (at the end of the fourth cycle) equal to 2.8 MPa for the pressure and 75% for the fission gas release. Compared to GERMINAL, pre-INSPYRE TRANSURANUS predicts a much lower FGR and consequently pin pressure in the fuel-cladding gap (Figs. 7 and 8 – right). Also, the evolution during the four irradiation cycles shows some differences, i.e., the peak FGR (slightly more than 30%) is predicted during the first cycle, then slightly decreases to 30% at the end of irradiation. The corresponding maximum value of the pin pressure reached at the end of irradiation is around 1.25 MPa, which is lower than the typical end-of-life values predicted for fast reactor pins (e.g., in the case of the irradiation experiments considered in INSPYRE [41,42]). The evolution of the fuel temperature regime predicted by pre-INSPYRE TRANSURANUS (Fig. 6 – right), which is the main driver of the fission gas release, limits the FGR (and corresponding gap pressure) from the middle of the first power cycle on when it steadily decreases as explained above. As a result, both FGR and pressure results from pre-INSPYRE TRANSURANUS are lower compared to expected predictions on FR fuel pins (e.g., FGR ~ 75% from heterogeneous fuel columns).

The post-INSPYRE GERMINAL result is significantly different from the reference one in terms of FGR dynamics (Fig. 7 – left), reflecting on the pin pressure evolution (Fig. 8 – left), although the end-of-irradiation value is only slightly lower (~ 72%). The SCIANTIX fission gas behaviour model [10,36] coupled to GERMINAL leads to a lower FGR rate during the nominal power cycles, contributing to the decrease of the integral FGR, and to sudden FGR bursts during the inter-cycles, essentially during the reactor shutdown phases. This dynamics during the steady-state reactor operation is linked to the coupling artifact mentioned in Section 2, i.e., the current modelling of the evolution of the open paths for fission gas release from the pellets, allowing for the accumulation of fission gases at the grain boundaries after a burst release effect. Hence, the FGR is limited during a power cycle until the threshold for the storing capability of the grain boundaries is reached again, triggering the fission gas release again during a power cycle of normal operation. This is evident from the grey line in Fig. 7 - left towards the end of the second cycle, when the FGR starts to increase again. This FGR

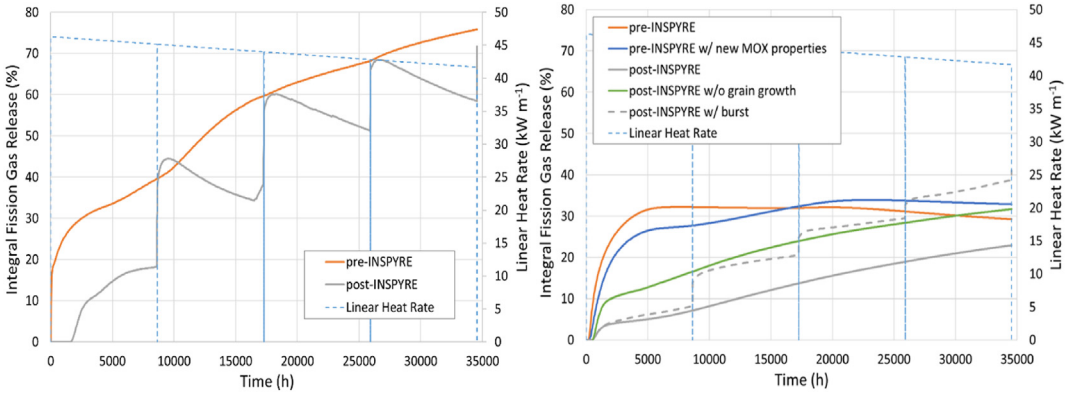

Fig. 7. Integral fission gas release evolution as predicted by GERMINAL (left) and TRANSURANUS (right).

behaviour has a direct impact on the fuel pin inner pressure, characterized by consequent pressure jumps between power cycles. Coherently with the integral fission gas release, which is not interrupted during the power cycles of reactor operation, the pressure in the gap continuously increases but with a lower rate compared to the burst release events. The TRANSURANUS post-INSPYRE simulation provides a lower integral FGR and pin inner pressure (maximum values around 23% and 1.2 MPa, respectively), both compared to pre-INSPYRE TRANSURANUS and to GERMINAL. This is not the effect of the novel correlations for the MOX properties [11,37–39] since they provide a FGR behaviour similar to the pre-INSPYRE one, with higher FGR and gap pressure at the end-of-irradiation, mainly due to the stronger degradation with burn-up of the novel thermal conductivity which reflects in higher fuel temperatures enhancing the fission gas dynamics. The reason for the dumped fission gas-related results is identified in the current fuel grain growth model available in TRANSURANUS [10,27,43], which is tailored on LWR irradiation conditions and does not feature an upper limit for the grain size. The application of the present model to fast reactor irradiation conditions hence prevents a FGR typical of fast reactor fuel pins. This supports the need of performing a sensitivity analysis on the fuel grain growth model, whose results are also shown in the previous (and following) figures. The green curves of Figs. 7 and 8 show how both results are higher than the pre-INSPYRE ones (predicted end-of-irradiation values of 31% for the FGR and ~ 1.5 MPa for the pin inner pressure) if the grain growth model is switched off in the post-INSPYRE simulation. The sensitivity of the FGR and pin pressure results to the burst releases of inter-granular fission gas from the fuel to the fuel-cladding gap has been tested by activating the novel burst release model implemented in SCIANTIX [10,17] (post-INSPYRE simulations). The effect consists in sudden step increases of both FGR and pin pressure during the inter-cycles (Figs. 7 and 8 – right, respectively), like those observed also from GERMINAL simulations, leading to the highest final values of pin pressure around 1.83 MPa and FGR around 41%. These outcomes reveal more consistent with the GERMINAL ones and more representative of values expected from the operation of FR fuel pins. Despite the sensitivity analyses performed with TRANSURANUS, the simulation results in terms of both FGR and pin inner pressure reveal still strongly different, and therefore identify open points concerning the safety assessment of heterogeneous pins designed for irradiation in the ASTRID reactor and the different strategies adopted by the two codes for the coupling with the SCIANTIX mechanistic fission gas behaviour module. A more detailed analysis and interpretation of the mechanism of burst release of fission gases, as simulated by the SCIANTIX module, is provided in the following Section 5.

4.3. Axial profiles: fuel central temperature and fuel-cladding gap width

The axial profiles of the fuel central temperature predicted by both codes, shown in Fig. 9, are clearly correlated to the peculiar axial profile of the linear power of the heterogeneous fissile-fertile fuel column. The impact of the INSPYRE models (post-INSPYRE code versions) is visible especially on the TRANSURANUS results (Fig. 9 – right), reflecting the adoption of the novel thermal conductivity correlation [38] but also of the SCIANTIX module coupled to TRANSURANUS [10,11], whose effect depends on the fuel grain growth modelling. If no grain growth is considered besides the

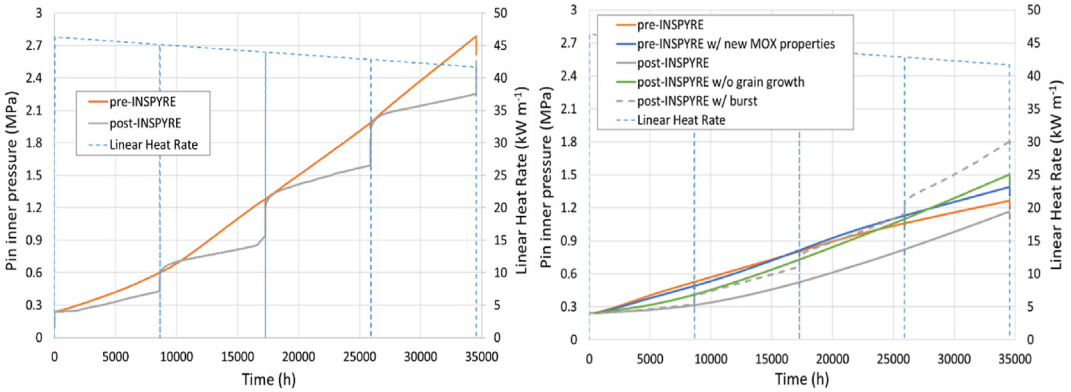

Fig. 8. Fuel pin inner pressure evolution as predicted by GERMINAL (left) and TRANSURANUS (right).

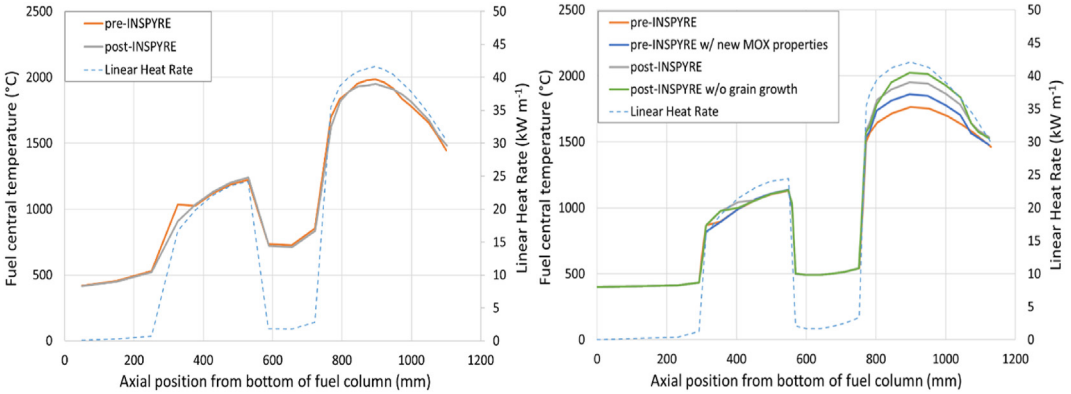

Fig. 9. Axial profiles of the fuel central temperature at the end of the fourth irradiation cycle, as predicted by GERMINAL (left) and TRANSURANUS (right).

post-INSPYRE modelling options, smaller fuel grains imply a higher fission gas diffusion to the grain boundaries, and consequently a higher fission gas release in the fuel-cladding gap. This results in higher fuel temperatures (coherently with the evolution in time shown by Fig. 6 – right) caused by a lower gap conductance, since the gap composition is more polluted by fission gases.

The axial profiles of fuel-cladding radial gap size at the beginning of irradiation (Fig. 10, just after the reactor start-up) are strictly related to the axial profile of the linear power as they are driven by the fuel and cladding relative thermal expansions, for both codes and both pre- and post-INSPYRE code versions (providing similar results). The gap after the first reactor start-up is slightly wider according to the GERMINAL predictions, i.e., ~ 20 μm higher in the upper fissile zone of the column (around the peak power node). Although limited, the effect of the novel correlation for the MOX fuel thermal expansion [11,37] in TRANSURANUS is visible from Fig. 10 – right, i.e., determining a slightly lower gap width than the pre-INSPYRE one in the hotter (upper) part of the fuel column. Considering the gap width axial profiles predicted by pre-INSPYRE codes at the end of irradiation (Fig. 11), the gap size is reduced in the fertile zones of the active column, while fuel-cladding contact occurs in the fissile zones (only partially in the lower fissile zone where the power is lower). According to GERMINAL, the gap is opened at the end of the fourth irradiation cycle in the upper fissile zone due to the presence of the JOG layer formed between the pellets and the cladding [5] (coherently with the gap evolution in time shown by Fig. 5 – left, Section 4.1).

The post-INSPYRE GERMINAL code predicts a different (lower) gap re-opening due to the JOG in the upper fissile zone of the active column, at the end of irradiation (Fig. 11 – left), due to a different caesium migration and release in the fuel-cladding gap predicted by means of the inert gas model implemented in the SCIANTIX module, leading to a different estimation of the JOG thickness (namely, lower). Instead, according to post-INSPYRE TRANSURANUS (Fig. 11 – right), the gap is completely closed in the upper zone of the pin (where the linear power values are the highest, axially), while the gap is only partially closed in the lower fissile zone at the end of irradiation. Both the TRANSURANUS post-INSPYRE results (also preventing the fuel grain growth), compared to the pre-INSPYRE one, show wider predicted gap sizes in the lower fissile zone which result in locally higher fuel central temperatures, as shown by Fig. 9 – right. The wider fuel-cladding gap size is determined by the fuel swelling provided by SCIANTIX in that axial zone of the fuel column, i.e., a locally lower fuel swelling with respect to what predicted by pre-INSPYRE TRANSURANUS (according to an empirical, burn-up driven correlation [44]), mainly due to the lower linear power and temperatures experienced by the fuel in the lower fissile zone. The consequent limited diffusion of the produced fission gas to the grain boundaries limits the (dominant) contribution of inter-granular bubbles to fuel swelling, according to the SCIANTIX modelling coupling mechanistic fission gas behaviour and swelling.

4.4. Axial profiles: cladding swelling

The axial profiles of cladding swelling predicted by the

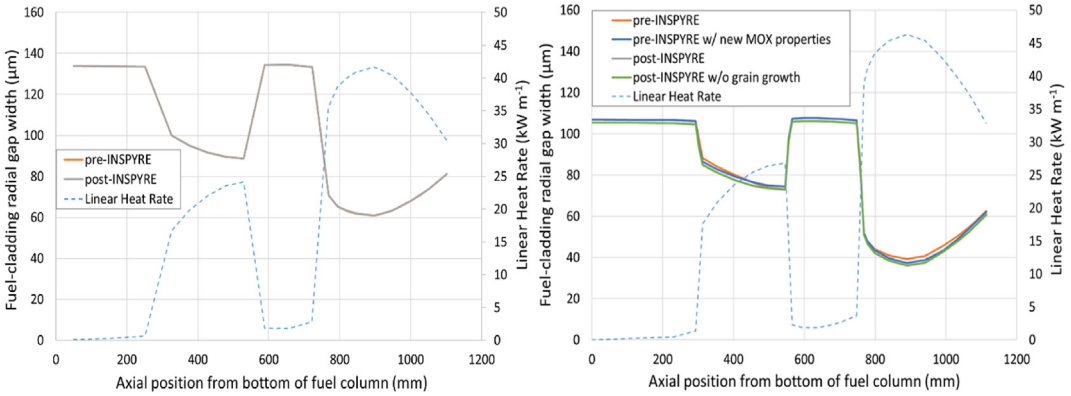

Fig. 10. Axial profiles of the pellet-cladding gap width at the beginning of the first irradiation cycle, as predicted by GERMINAL (left) and TRANSURANUS (right).

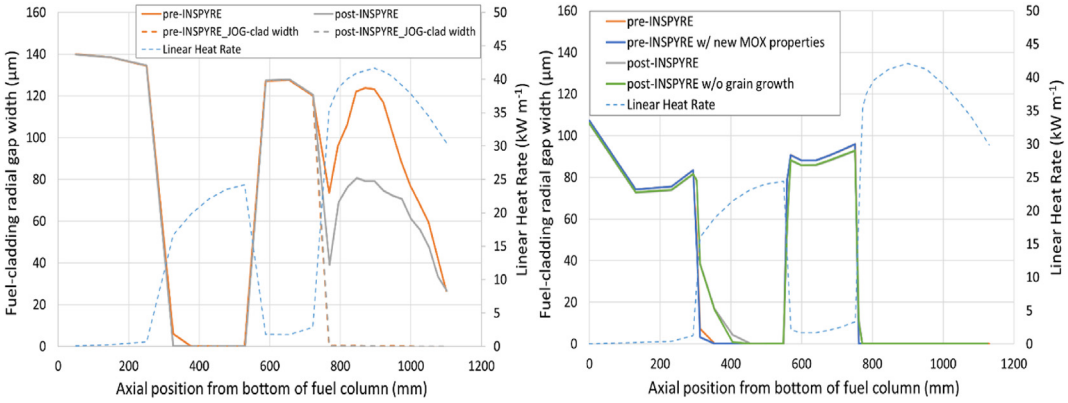

Fig. 11. Axial profiles of the pellet-cladding gap width at the end of the fourth irradiation cycle, as predicted by GERMINAL (left) and TRANSURANUS (right).

GERMINAL and TRANSURANUS codes at the end of the fourth power cycle (Fig. 12) correspond to similar shapes, although they are substantially different in values. It is worth noting that the swelling profile predicted by TRANSURANUS is mainly driven by the axial pin power, with the peak of swelling in the lower part of the upper fissile zone (at an axial position slightly below the peak power node), due to the combination of high fast neutron fluence and cladding temperature in the critical range for the swelling of 15–15Ti. GERMINAL provides a consistent prediction determined by the dose damage rate on the cladding counterbalanced by an annealing rate induced by the temperature. The cladding swelling is much more pronounced as predicted by TRANSURANUS, according to the best-estimate correlation recommended in the code for 15-15Ti austenitic stainless steels (the ASTRID cladding material according to the current pin design), reported in Ref. [45]. A higher swelling is coherent with a higher cladding outer radius than the one calculated by GERMINAL. Although both codes employ swelling models tailored on 15-15Ti steel data, the two correlations differ e.g., in the temperature and dose thresholds triggering the swelling, or also in the dependency on the irradiation damage. These prove to be the main causes of discrepancies in the cladding swelling predictions provided by the two codes. Nevertheless, the same axial shape of the volumetric swelling at the end of irradiation suggests a deeper joint investigation of the dependences of the GERMINAL and TRANSURANUS models on the cladding damage (dpa) or on the neutron fluence. The cladding swelling profile proves to be slightly affected by the choice of the novel INSPYRE correlations for MOX fuel properties, which have only an indirect influence by affecting the predicted fuel-cladding gap width and consequently the calculated temperature on the cladding inner bound, that may deviate from the peak temperature for the enabling of swelling. A maximal swelling value of around 1.7% is predicted by GERMINAL, while ~ 5.5% is obtained at most by TRANSURANUS (from the post-INSPYRE simulation with the fuel grain growth switched off). Besides the stress-free strain nature of the irradiation swelling of the cladding, driven by the local temperature and fast neutron fluence, the cladding radial deformation is also directly impacted by stress-dependent creep due to FCMI (Fuel-Cladding Mechanical Interaction) when gap closure occurs. This effect, determined mainly by fuel thermal expansion and swelling due to retained fission gases, and resulting in significant contact pressures on the cladding inner surface, proves to be particularly relevant from TRANSURANUS calculations (while limited in GERMINAL due to the JOG layer between fuel and cladding implying a softer fuel-cladding contact).

5. Further insights on the fission gas behaviour: burst release effects

Since this work focuses on the inclusion of SCIANTIX as a fission gas behaviour module in both GERMINAL and TRANSURANUS fuel performance codes, it is worth to provide a deeper interpretation of the peculiar kinetics of fission gas release observed in the post-INSPYRE simulations performed with both codes, i.e., the steep (burst) increases of fission gas release and related pin inner pressure between the irradiation cycles (Figs. 7 and 8).

Fig. 13 provides a zoom on the first ASTRID reactor shutdown, occurring between the first and the second irradiation cycle. The

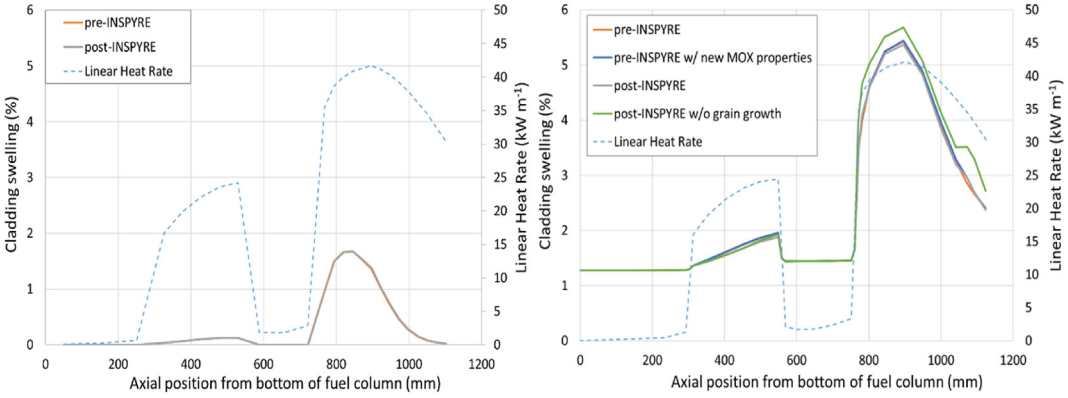

Fig. 12. Axial profiles of the cladding swelling at the end of the fourth irradiation cycle, as predicted by GERMINAL (left) and TRANSURANUS (right).

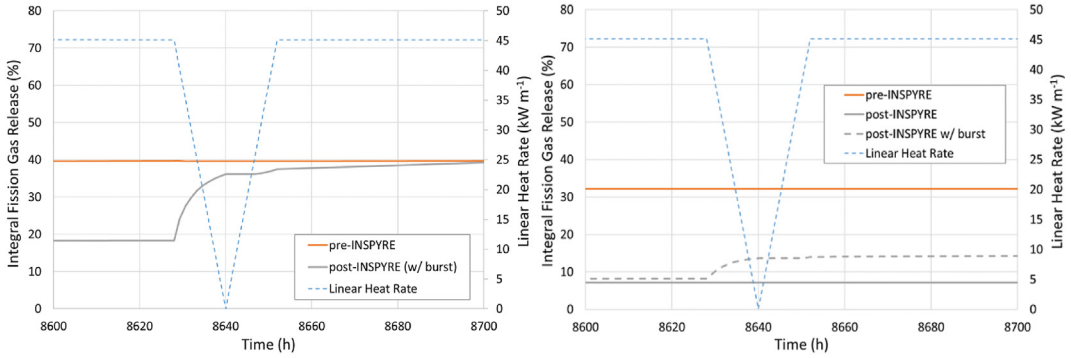

Fig. 13. Integral fission gas release evolution, zoomed on the inter-cycle between the first and the second irradiation cycles, as predicted by GERMINAL (left) and TRANSURANUS (right). The post-INSPYRE GERMINAL result already accounts for the SCIANTIX burst release model, while an additional sensitivity considering the burst release modelling is performed with TRANSURANUS ("post-INSPYRE w/burst"). For the complete evolution of the integral fission gas release, see Fig. 7.

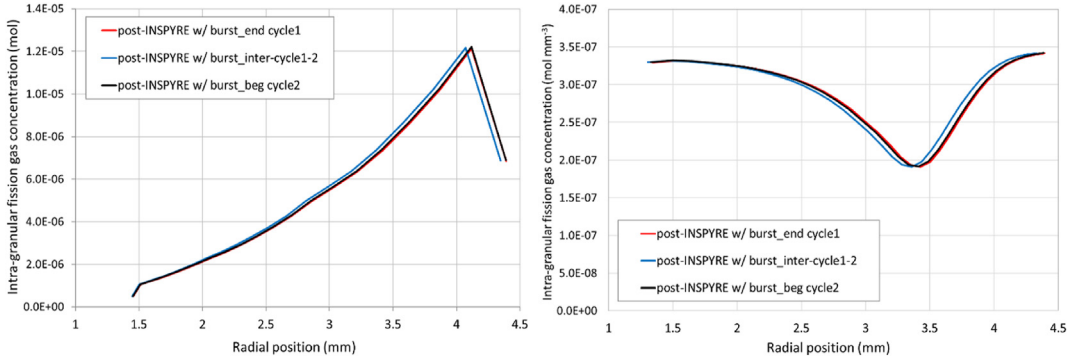

Fig. 14. Radial profiles of the intra-granular fission gas concentration at the axial peak power node, at different times representative of the inter-cycle between the first and the second irradiation cycles, as predicted by GERMINAL (left, in mol) and TRANSURANUS (right, in mol mm^{-3}).

increase in the fission gas release occurs mainly along the power transient down, with a more limited contribution provided by the subsequent heat-up transient. Besides the quantitative difference between GERMINAL//SCIANTIX and TRANSURANUS//SCIANTIX, the predicted trend is common to both codes. This behaviour represents an extension of the results obtained by Barani et al. [17], who performed a cross-validation of BISON [46] and an earlier version of TRANSURANUS.

Figs. 14 and 15 shed light on the physics-based mechanism to which the burst release kinetics is ascribed, i.e., the micro-cracking of grain boundaries [17,47,48]. The model currently available in SCIANTIX is based on a semi-empirical approach, involving a micro-cracking function $m(T)$ tailored on data from separate-effect experiments. The model acts by reducing the fractional coverage F, i.e., the surface porosity on grain faces, during each temperature transient, through the variation of the intact fraction of grain faces f, according to:

$$\frac{\mathrm{d}f}{\mathrm{d}t} = -\frac{\mathrm{d}m}{\mathrm{d}T}\frac{\mathrm{d}T}{\mathrm{d}t}f \tag{1}$$

$$\frac{\mathrm{d}F}{\mathrm{d}t} = \frac{\mathrm{d}f}{\mathrm{d}t}F \tag{2}$$

Thus, each temperature transient $\mathrm{d}T/\mathrm{d}t$ progressively reduces the fraction of intact grain faces, and by consequence the fractional coverage linked to the amount of gas stored at the grain boundaries, triggering a burst contribution to the fission gas release. Each temperature variation is empirically weighted by the local temperature derivative of the micro-cracking function $\mathrm{d}m/\mathrm{d}T$. The micro-cracking function m is defined as non-symmetrical during heating and cooling transients, exhibiting higher fission gas release during cooling, in agreement with the available experimental data provided by Ref. [49][2] and accounted for by Ref. [17]. Moreover, it is defined to trigger the maximum gas release around a specific central temperature, which is ~ 1500°C and defined as a function of the local fuel burn-up. Although the burst release model herein described is based and validated on LWR data, it is deemed extendable to FR fuels since it involves the micro-cracking of grain boundaries determined by power (and temperature) transients. The high power rates typical of fast reactors during base irradiation, and the strong power variations during FR inter-cycles (power shutdown and start-up), are favourable conditions for burst releases to occur also in FR fuels, considering the micro-structural differences with respect to LWR fuels (e.g., the significant amount of paths for fission gas release formed in the early stages of irradiation). An adjustment of the parameters of the burst release model for its application to FR fuels has not been performed at this stage, given the lack of dedicated data/indications in the current literature. This, together with the results presented in Section 4 (Figs. 7 and 8 in particular), opens the need for a revision of the model targeting specific FR materials and applications, by e.g., acting on the temperature triggering the burst release or allowing a direct release of fission gas to the fuel-cladding gap in light of the typically well-developed microstructure of FR fuels (in terms of

[2] The referenced, currently available data were obtained from light water reactor fuel subjected to power ramps (hence, thermal reactor irradiation conditions) or to annealing tests up to 1800 °C [49].

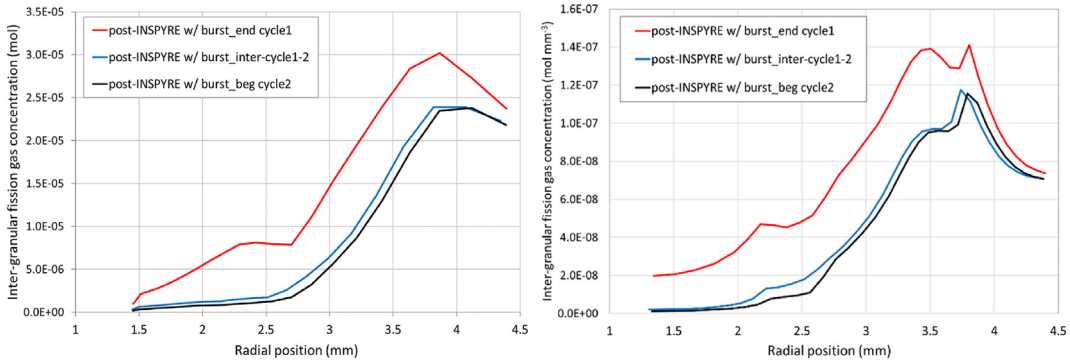

Fig. 15. Radial profiles of the inter-granular fission gas concentration at the axial peak power node, at different times representative of the inter-cycle between the first and the second irradiation cycles, as predicted by GERMINAL (left, in mol) and TRANSURANUS (right, in mol mm^{-3}).

restructuring and porosity, as shown e.g., by Refs. [50,51]). The availability of novel data, either experimental or from micro-scale calculations, would be highly beneficial to support further modelling advancements.

Figs. 14 and 15, showing the radial profiles of xenon concentration predicted by SCIANTIX inside the fuel grains and at the grain boundaries, respectively, confirm that the observed fission gas release kinetics are indeed ascribed to the micro-cracking of grain boundaries. The evolution of the xenon radial profiles along the inter-cycle between the first and the second irradiation cycles (but similarly occurring during every ASTRID inter-cycle) clearly shows that almost no additional transfer of gas from inside the grains to the grain boundaries is predicted, whereas the amount of gas at the grain boundaries decreases, i.e., is released. In particular, the release occurs mainly during the cool down transient, as imposed by the non-symmetrical formulation of the micro-cracking function [17,47,48].

6. Conclusions and future development paths

A benchmark between the GERMINAL and TRANSURANUS fuel performance codes has been proposed and performed on the Gen-IV sodium-cooled ASTRID case study, considering an axially heterogeneous fuel pin featuring fertile and fissile fuel zones (i.e., UO_2 and (U, Pu)O_2 fuel pellets, respectively). The simulation results in terms of integral pin performance indicators have been presented and discussed as obtained by both codes, in their reference state-of-the-art versions ("pre-INSPYRE") and corresponding to their extended versions ("post-INSPYRE") in which the novel models for MOX fuel properties and for fission gas behaviour (via SCIANTIX), developed in the framework of the INSPYRE Project, have been implemented.

The herein performed analysis of the code simulation outcomes is devoted to the main quantities and processes related to two engineering design criteria fundamental for the pin safety under irradiation, i.e., the margin to fuel melting and the cladding integrity. In particular, the focus is on the predicted fuel maximal temperature and on the pin inner pressure evolution as resulting from the physics-based description of fission gas behaviour and release in the fuel-cladding gap provided by the SCIANTIX code, coupled as a module to both GERMINAL and TRANSURANUS. Moreover, the impact on the fission gas release and related gap pressure of the fuel micro-cracking and burst release model provided by SCIANTIX is assessed for the first time under fast reactor irradiation conditions.

From the comparison and assessment of pre-INSPYRE and post-INSPYRE code results, a first conclusion concerns the SCIANTIX modelling leading to different fission gas release kinetics from GERMINAL or TRANSURANUS (already dissimilar as calculated by the reference code versions). The SCIANTIX fission gas behaviour predictions are strongly related to the modelling of fuel grain growth, currently tailored on LWR fuel data in TRANSURANUS, and underline the importance of a coherent description of the micro-structure evolution in MOX fuels for fast reactor applications for a properly-working physics-based description. This work clearly allows to identify that the current overestimations of the FR MOX grain growth lead, especially in the restructured zone of the fuel, to an increase of the intra-granular gas diffusion time, consequently increasing the gas predicted as retained into the fuel pellets and decreasing significantly the calculated gas release in the fuel-cladding gap. Additional modelling efforts should focus on the onset of FGR at beginning of life predicted by SCIANTIX, currently providing a fission gas incubation time in the fuel. Also, the effects of the rapid micro-structure evolution of FR MOX after reactor start-up need to be targeted, to achieve a FGR kinetics more consistent with that expected after the first power ramp under FR irradiation conditions (i.e., with the pre-INSPYRE code predictions herein reported, see also [41]).

Another highlight of this work concerns the prediction of burst releases of inter-granular gas during power transients of reactor start-up/shutdown, made available by the SCIANTIX module and representing a step forward in the extension of fuel performance codes with respect to their reference versions. A deep interpretation of the burst release effects on the fission gas release and related pin inner pressure, as provided by SCIANTIX coupled to both fuel performance codes and occurring prevalently during power shutdown ramps, is herein proposed. The burst releases predicted during the shutdown phases at the end of each ASTRID irradiation cycle, step-increasing the fission gas release and gap pressure, are linked to the SCIANTIX modelling of fuel micro-cracking, leading to the release of the inter-granular fission gases accumulated in that fuel region during the previous power cycle. Despite the clear need of further extension and validation of the SCIANTIX module targeting phenomena typical of fast reactor fuels, its coupling with fuel performance codes and the first results herein presented pave the way towards a reliable representation of the fission gas dynamics in FR pins on a mechanistic basis.

The first application of fuel performance codes and of the coupled SCIANTIX module to predictions of fission gas dynamics in the ASTRID SFR case study, performed and discussed in this work, suggests various future development paths, needed by the current codes to continuously improve their predictive capabilities towards fast reactor fuels and irradiation conditions. Following the focus on fission gas-related results, surely the implementation in codes of an appropriate model for the grain growth of fast reactor MOX fuels is essential, reflecting in higher fission gas release predictions as

expected from the high temperatures experienced by fuels under fast neutron spectrum. The SCIANTIX mechanistic description of fission gas behaviour would benefit from e.g., a limited grain growth as a starting point for further modelling refinements, in absence of dedicated in-pile data measured on fast reactor fuels with increasing burn-up. Moreover, dedicated efforts and knowledge are required to extend the modelling and validation of the fission gas burst releases, currently tailored on light water (thermal) reactor fuel and conditions on which data are available at present. The authors are aware that the representativeness of the burst release model herein presented can be improved for what concerns the ASTRID pin irradiation conditions (experiencing stronger power transient, in principle enhancing the micro-cracking effect), despite the generally valid physics-based approach adopted in SCIANTIX and introduced in the fuel performance code framework. The parameters of the FGR and burst release model of SCIANTIX are open to be updated as soon as additional experimental data or lower-length scale information will become available, to improve the model suitability for fast reactor MOX. Further important modelling extensions of fuel performance codes can be identified from this benchmark activity. An additional needed development concerns the introduction in TRANSURANUS of a model for the JOG formation and evolution in the fuel-cladding gap, to harmonize the predicted evolution of the gap width at high burn-up and to account for both the JOG thermal feedback on the fuel and its effect on the fuel-cladding mechanical interaction. Furthermore, the consideration in the SCIANTIX module of the grain boundary sweeping effect, associated to the restructuring of FR fuels and contributing significantly to the fission gas release, is planned towards a more comprehensive description of the intergranular dynamics.

Besides the identified open needs from the modelling point of view, additional analyses to complete the safety assessment process are necessary and of interest in perspective. For what concerns specifically the ASTRID case study, the path forward foresees the consideration of specific design limits on the ASTRID pin behaviour, not introduced in the present work (although the discussion focused on integral simulation outcomes related to the pin safety under irradiation). As already mentioned, these design criteria should concern primarily an upper limit on the maximal fuel temperature and allowed cladding stress levels/visco-plastic strain, in order to avoid pin failures related to fuel melting or loss of integrity of the cladding. Lastly, extending the present case study (devoted to normal operation conditions) accounting for operational transients or accidental conditions is required to demonstrate in full the safety of SFR reactors and of Generation IV concepts in general.

Declaration of competing interest

The authors declare that they have no known competing financial interests or personal relationships that could have appeared to influence the work reported in this paper.

Acknowledgments

This work has received funding from the Euratom research and training programme 2014–2018 through the INSPYRE project under grant agreement No 754329.

References

[1] GIF (Generation IV International Forum), GIF R&D Outlook for Generation IV Nuclear Energy Systems - 2018 Update, 2018.
[2] GIF (Generation IV International Forum), Annual Report 2020, 2020.
[3] T. Beck, V. Blanc, J.-M. Escleine, D. Haubensack, M. Pelletier, M. Phelip, B. Perrin, C. Venard, Conceptual design of ASTRID fuel sub-assemblies, Nucl. Eng. Des. 315 (2017) 51–60.
[4] C. Venard, C. Coquelet-Pascal, A. Conti, D. Gentet, P. Lamagnère, R. Lavastre, P. Gauthé, B. Bernardin, T. Beck, D. Lorenzo, A.-C. Scholer, B. Perrin, D. Verrier, in: The ASTRID Core at the End of the Conceptual Design Phase, FR17, 2017, 26-29 June, Yekaterinburg, Russia.
[5] M. Lainet, B. Michel, J.C. Dumas, M. Pelletier, I. Ramière, GERMINAL, a fuel performance code of the PLEIADES platform to simulate the in-pile behaviour of mixed oxide fuel pins for sodium-cooled fast reactors, J. Nucl. Mater. 516 (2019) 30–53.
[6] B. Michel, I. Ramière, I. Viallard, C. Introini, M. Lainet, N. Chauvin, V. Marelle, A. Boulore, T. Helfer, R. Masson, J. Sercombe, J.C. Dumas, L. Noirot, S. Bernaud, Two fuel performance codes of the PLEIADES platform: ALCYONE and GERMINAL, in: J. Wang, X. Li, C. Allison, J. Hohorst (Eds.), Nuclear Power Plant Design and Analysis Codes - Development, Validation and Application Chap. 9, Woodhead Publishing Series in Energy, Elsevier, 2021, pp. 207–233.
[7] K. Lassmann, TRANSURANUS: a fuel rod analysis code ready for use, J. Nucl. Mater. 188 (C) (1992) 295–302.
[8] A. Magni, A. Del Nevo, L. Luzzi, D. Rozzia, M. Adorni, A. Schubert, P. Van Uffelen, The TRANSURANUS fuel performance code, in: J. Wang, X. Li, C. Allison, J. Hohorst (Eds.), Nuclear Power Plant Design and Analysis Codes - Development, Validation and Application Chap. 8, Woodhead Publishing Series in Energy, Elsevier, 2021, pp. 161–205.
[9] D. Olander, Fundamental Aspects of Nuclear Reactor Fuel Elements, California University, Department of Nuclear Engineering, Berkeley, CA, USA, 1976.
[10] D. Pizzocri, T. Barani, L. Luzzi, SCIANTIX: a new open source multi-scale code for fission gas behaviour modelling designed for nuclear fuel performance codes, J. Nucl. Mater. 532 (2020), 152042.
[11] P. Van Uffelen, A. Schubert, L. Luzzi, T. Barani, A. Magni, D. Pizzocri, M. Lainet, V. Marelle, B. Michel, B. Boer, S. Lemehov, A. Del Nevo, Incorporation and verification of models and properties in fuel performance codes, INSPYRE Deliverable D7.2 (2020).
[12] P. Le Coz, J.F. Sauvage, J.P. Serpantie, Sodium-cooled fast reactors: the ASTRID plant project1, in: Proceedings of ICAPP 201, 2011.
[13] B. Faure, P. Archier, J.-F. Vidal, J.M. Palau, L. Buiron, Neutronic calculation of an axially heterogeneous ASTRID fuel assembly with APOLLO3®: analysis of biases and foreseen improvements, Ann. Nucl. Energy 115 (2018) 88–104.
[14] C. Venard, T. Beck, B. Bernardin, A. Conti, D. Gentet, P. Lamagnere, P. Sciora, D. Lorenzo, A. Tosello, M. Vanier, A.-C. Scholer, D. Verrier, F. Barjot, D. Schmitt, The ASTRID core at the midterm of the conceptual design phase (AVP2), in: ICAPP 2015 - International Congress on Advances in Nuclear Power Plants, 3-5 May 2015, Nice, France, 2015.
[15] EERA-JPNM, INSPYRE - Investigations Supporting MOX Fuel Licensing in ESNII Prototype Reactors [Online]. Available: http://www.eera-jpnm.eu/inspyre/, 2017.
[16] L. Luzzi, T. Barani, A. Magni, D. Pizzocri, A. Schubert, P. Van Uffelen, V. Marelle, B. Michel, B. Boer, S. Lemehov, A. Del Nevo, Definition of Detailed Configurations of the Case Studies for the Fuel Performance Simulations in Task 7.3, INSPYRE Milestone MS16, 2019.
[17] T. Barani, E. Bruschi, D. Pizzocri, G. Pastore, P. Van Uffelen, R.L. Williamson, L. Luzzi, Analysis of transient fission gas behaviour in oxide fuel using BISON and TRANSURANUS, J. Nucl. Mater. 486 (2017) 96–110.
[18] M. Pelletier, Y. Guerin, Fuel Performance of Fast Spectrum Oxide Fuel, in: Chap. 2.03, in: R.J.M. Konings, R.E. Stoller (Eds.), Comprehensive Nuclear Materials, 2, Elsevier, 2020, pp. 72–105.
[19] D. Pizzocri, T. Barani, L. Luzzi, SCIANTIX Code [Online]. Available: https://gitlab.com/poliminrg/sciantix, 2020.
[20] D. Pizzocri, G. Pastore, T. Barani, A. Magni, L. Luzzi, P. Van Uffelen, S.A. Pitts, A. Alfonsi, J.D. Hales, A model describing intra-granular fission gas behaviour in oxide fuel for advanced engineering tools, J. Nucl. Mater. 502 (2018) 323–330.
[21] G. Pastore, L. Luzzi, V. Di Marcello, P. Van Uffelen, Physics-based modelling of fission gas swelling and release in UO_2 applied to integral fuel rod analysis, Nucl. Eng. Des. 256 (2013) 75–86.
[22] L. Cognini, A. Cechet, T. Barani, D. Pizzocri, P. Van Uffelen, L. Luzzi, Towards a physics-based description of intra-granular helium behaviour in oxide fuel for application in fuel performance codes, Nucl. Eng. Technol. 53 (2) (2021) 562–571.
[23] A. Cechet, S. Altieri, T. Barani, L. Cognini, S. Lorenzi, A. Magni, D. Pizzocri, L. Luzzi, A new burn-up module for application in fuel performance calculations targeting the helium production rate in $(U,Pu)O_2$ for fast reactors, Nucl. Eng. Technol. 53 (6) (2021) 1893–1908.
[24] A. Scolaro, I. Clifford, C. Fiorina, A. Pautz, The OFFBEAT multi-dimensional fuel behavior solver, Nucl. Eng. Des. 358 (2020), 110416.
[25] A. Scolaro, Development of a Novel Finite Volume Methodology for Multi-Dimensional Fuel Performance Applications,, PhD Thesis,, EPFL, Switzerland, 2021.
[26] C. Sari, Grain growth kinetics in uranium-plutonium mixed oxides, J. Nucl. Mater. 137 (2) (1986) 100–106.
[27] J.B. Ainscough, B.W. Oldfield, J.O. Ware, Isothermal grain growth kinetics in sintered UO_2 pellets, J. Nucl. Mater. 49 (2) (1973) 117–128.
[28] P. Botazzoli, Helium Production and Behaviour in LWR Oxide Nuclear Fuels, PhD Thesis,, Politecnico di Milano, Italy, 2011.
[29] P. Botazzoli, L. Luzzi, S. Bremier, A. Schubert, P. Van Uffelen, Microstructural

evolution in heterogeneous and homogeneous MOX fuels, in: NuMat 2010 - the Nuclear Materials Conference, 2010, 4-7 October, Karlsruhe, Germany.
[30] F. Verdolin, S. Novascone, D. Pizzocri, G. Pastore, T. Barani, L. Luzzi, Modelling fission gas behaviour in fast reactor (U,Pu)O_2 fuel with BISON, J. Nucl. Mater. 547 (2021), 152728.
[31] G. Pastore, D. Pizzocri, C. Rabiti, T. Barani, P. Van Uffelen, L. Luzzi, An effective numerical algorithm for intra-granular fission gas release during non-equilibrium trapping and resolution, J. Nucl. Mater. 509 (2018) 687–699.
[32] M.S. Veshchunov, V.D. Ozrin, V.E. Shestak, V.I. Tarasov, R. Dubourg, G. Nicaise, Development of the mechanistic code MFPR for modelling fission-product release from irradiated UO_2 fuel, Nucl. Eng. Des. 236 (2) (2006) 179–200.
[33] M.S. Veshchunov, V.I. Tarasov, Modelling of irradiated UO_2 fuel behaviour under transient conditions, J. Nucl. Mater. 437 (1–3) (2013) 250–260.
[34] M.V. Speight, A calculation on the migration of fission gas in material exhibiting precipitation and Re-solution of gas atoms under irradiation, Nucl. Sci. Eng. 37 (1969) 180–185.
[35] J.A. Turnbull, The distribution of intragranular fission gas bubbles in UO_2 during irradation, J. Nucl. Mater. 38 (2) (1971) 203–212.
[36] D. Pizzocri, T. Barani, L. Cognini, L. Luzzi, A. Magni, A. Schubert, P. Van Uffelen, T. Wiss, Synthesis of the inert gas behaviour models developed in INSPYRE, INSPYRE Deliverable D6.4 (2020).
[37] S. Lemehov, New correlations of thermal expansion and Young's modulus based on existing literature and new data, INSPYRE Deliverable D6.3 (2020).
[38] A. Magni, T. Barani, A. Del Nevo, D. Pizzocri, D. Staicu, P. Van Uffelen, L. Luzzi, Modelling and assessment of thermal conductivity and melting behaviour of MOX fuel for fast reactor applications, J. Nucl. Mater. 541 (2020), 152410.
[39] A. Magni, L. Luzzi, P. Van Uffelen, D. Staicu, P. Console Camprini, P. Del Prete, A. Del Nevo, Report on the improved models of melting temperature and thermal conductivity for MOX fuels and JOG, INSPYRE Deliverable D6.2 version 2 (2020).
[40] Y. Philipponneau, Thermal conductivity of (U, Pu)O_{2-x} mixed oxide fuel, J. Nucl. Mater. 188 (1992) 194–197.
[41] L. Luzzi, T. Barani, B. Boer, L. Cognini, A. Del Nevo, M. Lainet, S. Lemehov, A. Magni, V. Marelle, B. Michel, D. Pizzocri, A. Schubert, P. Van Uffelen, M. Bertolus, Assessment of three European fuel performance codes against the SUPERFACT-1 fast reactor irradiation experiment, Nucl. Eng. Technol. 53 (2021) 3367–3378.
[42] B. Boer, J. Eysermans, S. Lemehov, L. Luzzi, T. Barani, L. Cognini, A. Magni, D. Pizzocri, A. Del Nevo, A. Schubert, P. Van Uffelen, M. Bertolus, M. Lainet, V. Marelle, B. Michel, Report describing the results of the benchmark between improved codes and previous versions on selected experimental cases, INSPYRE Deliverable D7.3 (2021).
[43] P. Van Uffelen, P. Botazzoli, L. Luzzi, S. Bremier, A. Schubert, P. Raison, R. Eloirdi, M.A. Barker, An experimental study of grain growth in mixed oxide samples with various microstructures and plutonium concentration, J. Nucl. Mater. 434 (1–3) (2013) 287–290.
[44] W. Dienst, I. Muelle-Lyda, H. Zimmermann, Swelling, densification and creep of oxide and carbide fuels under irradiation, in: International Conference on Fast Breeder Reactor Performance, 1979, 5-8 March, Monterey, CA, USA.
[45] L. Luzzi, A. Cammi, V. Di Marcello, S. Lorenzi, D. Pizzocri, P. Van Uffelen, Application of the TRANSURANUS code for the fuel pin design process of the ALFRED reactor, Nucl. Eng. Des. 277 (2014) 173–187.
[46] R.L. Williamson, K.A. Gamble, D.M. Perez, S.R. Novascone, G. Pastore, R.J. Gardner, J.D. Hales, W. Liu, A. Mai, Validating the BISON fuel performance code to integral LWR experiments, Nucl. Eng. Des. 301 (2016) 232–244.
[47] D. Pizzocri, G. Pastore, T. Barani, E. Bruschi, L. Luzzi, P. Van Uffelen, Modelling of burst release in oxide fuel and application to the transuranus code, in: Proceedings Of the 11th International Conference WWER Fuel Performance, Modelling and Experimental Support, 2015, 28 September - 02 October, Varna, Bulgaria.
[48] G. Pastore, D. Pizzocri, J.D. Hales, S.R. Novascone, D.M. Perez, B.W. Spencer, R.L. Williamson, P. Van Uffelen, Modeling of transient fission gas behavior in oxide fuel and application to the BISON code, in: Proc. of Enlarged Halden Programme Group Meeting, 2015. Roros, Norway.
[49] K. Une, S. Kashibe, Fission gas release during post irradiation annealing of BWR fuels, J. Nucl. Sci. Technol. 27 (11) (1990) 1002–1016.
[50] F. Cappia, K. Tanaka, M. Kato, K. McClellan, J. Harp, Post-irradiation examinations of annular mixed oxide fuels with average burnup 4 and 5% FIMA, J. Nucl. Mater. 533 (2020), 152076.
[51] R.J. Parrish, F. Cappia, A. Aitkaliyeva, Comparison of the radial effects of burnup on fast reactor MOX fuel microstructure and solid fission products, J. Nucl. Mater. 531 (2020), 152003.